

Supplementary information for

Electrolytic cement clinker precursor production sustained through orthogonalization of ion vectors

Zishuai Zhang¹, Aubry S. R. Williams¹, Shaoxuan Ren¹, Benjamin A.W. Mowbray¹, Colin T. E. Parkyn¹,
Yongwook Kim¹, Tengxiao Ji¹, and Curtis P. Berlinguette^{1,2,3,4*}

¹Department of Chemistry, The University of British Columbia, 2036 Main Mall, Vancouver, British Columbia, V6T 1Z1, Canada.

²Department of Chemical and Biological Engineering, The University of British Columbia, 2360 East Mall, Vancouver, British Columbia, V6T 1Z3, Canada.

³Stewart Blusson Quantum Matter Institute, The University of British Columbia, 2355 East Mall, Vancouver, British Columbia, V6T 1Z4, Canada.

⁴Canadian Institute for Advanced Research (CIFAR), 661 University Avenue, Toronto, M5G 1M1, Ontario, Canada.

*Corresponding author: Curtis P. Berlinguette (cberling@chem.ubc.ca)

Experimental procedures

Materials

The bipolar membrane (BPM, Fumasep FBM) was purchased from the Fuel Cell Store. Nickel foam was purchased from MTI corporate. N₂ (99%), CO₂ (99%), and Ar (99.999%) gas were obtained from Praxair Canada Inc. Fumasep FBM was soaked in 1 M NaCl for 24 hours before use.

Ca²⁺ blocking CEM synthesis

The membrane modifications were performed in a beaker containing the reagents, leading to a two-face modification. The protons of the Nafion™ membrane were first ion-exchanged with protonated aniline using a 1 vol% aniline in 1 M HCl aqueous solution. After rinsing, the beaker was then filled with a 0.2 M K₂S₂O₈ aqueous solution to induce the polymerization for one hour. The Ca²⁺ blocking membranes were stored in 1 M HCl for a minimum of 24 hours prior to use.

Charge carried by K⁺

Inductively coupled plasma optical emission spectrometry (ICP-OES) was conducted on a Varian 725-ES. We evaluated the charge carried by K⁺ ions through a composite membrane by eqns (S1) and (S2). This value represents how effectively a composite membrane can block Ca²⁺ from passing through. A larger charge value carried by K⁺ suggests better exclusion of divalent (Ca²⁺) ions.

$$\text{Charge carried by K}^+ = \left(1 - \frac{[\text{Ca}^{2+}]_{\text{catholyte}}}{[\text{Ca}^{2+}]_{\text{theoretical value}}}\right) \times 100\% \quad (\text{S1})$$

$$[\text{Ca}^{2+}]_{\text{theoretical value}} = (I \times t) / 2F \quad (\text{S2})$$

where I is the operating current of the cement electrolyser, t is the electrolysis time, and F is the Faraday constant.

KCl recovery efficiency

We estimate the KCl recovery efficiency based on the volume of electrolyte before and after the filtration of Ca(OH)₂.

$$\text{KCl recovery efficiency} = \frac{V_{\text{filtrate}}}{V_{\text{electrolyte}}} \times 100\%$$

where V_{filtrate} is the volume of the filtrate, and $V_{\text{electrolyte}}$ is the volume of electrolyte before the filtration.

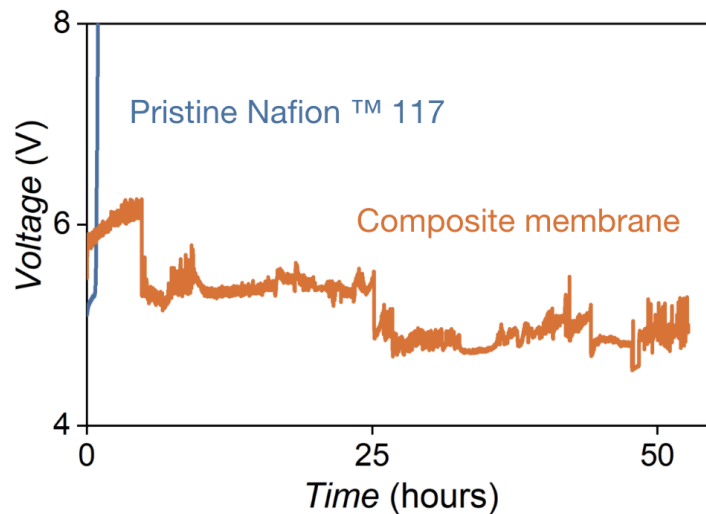


Figure S1. Cell voltage vs time of the cement electrolyser operating at 100 mA cm^{-2} with an unmodified Nafion™ 117 CEM (blue) and the PANI-coated composite membrane (orange). The cell voltage (V_{cell}) increases substantially after one hour of electrolysis with the pristine Nafion™ 117 due to precipitation of $\text{Ca}(\text{OH})_2$. The composite membrane is Nafion™ 117 with a 5–10 μm thick polyaniline (PANI) coating on each side. There is no voltage increase over time with the composite membrane because the PANI coating blocks the divalent Ca^{2+} cations and prevents them from precipitating in the cathode compartment.¹

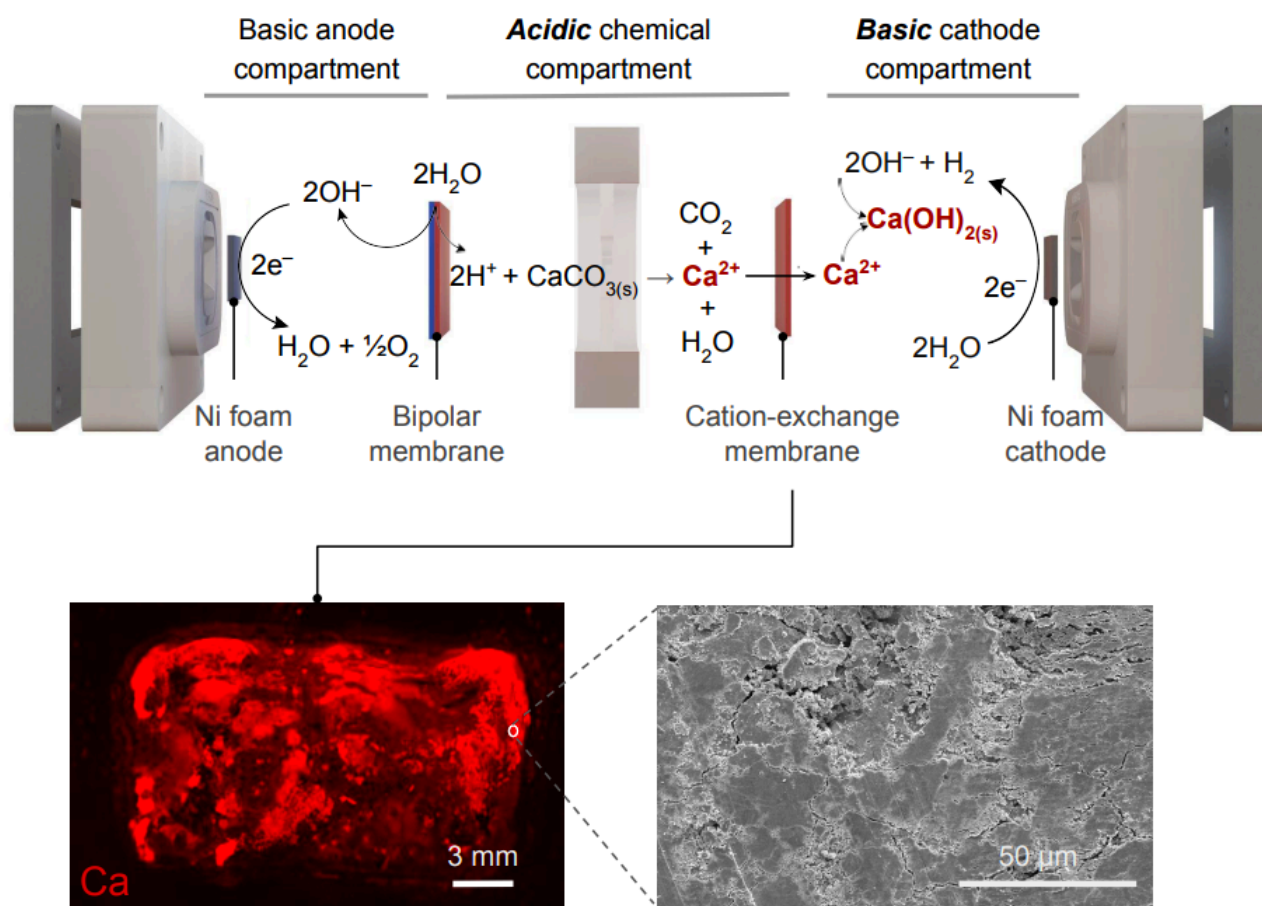


Figure S2. Ca(OH)_2 deposition on the cation-exchange membrane during electrolysis. Expanded view of the flow electrolyser reported in our previous work, which consists of anode, chemical, and cathode compartments. A BPM separates the anode and chemical compartments, and a CEM (NafionTM 117) separates the chemical and cathode compartments. Nickel foam was used as both the anode and cathode. Bottom line: XRF and SEM images of a NafionTM membrane after electrolysis at 100 mA cm^{-2} . Clusters of precipitated Ca(OH)_2 are observed on the surface of NafionTM after electrolysis.

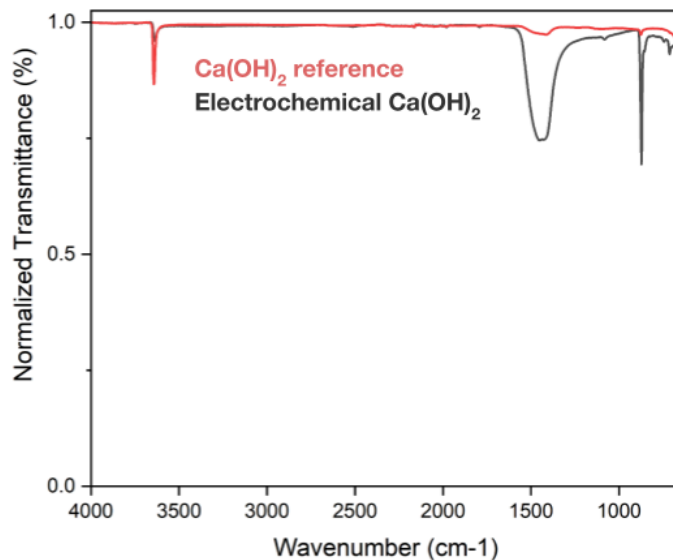


Figure S3. FTIR spectra of the electrochemically-produced cement clinker precursor (grey) and a Ca(OH)_2 reference (red). The intense peaks at $1,473$ and 918 cm^{-1} correspond to those observed in reference CaCO_3 FTIR spectra.² Missing peaks at $1,620$ and $2,164\text{ cm}^{-1}$ and no broad peak at $3,400\text{ cm}^{-1}$ suggest that CaCl_2 was not present in the electrochemical Ca(OH)_2 .³

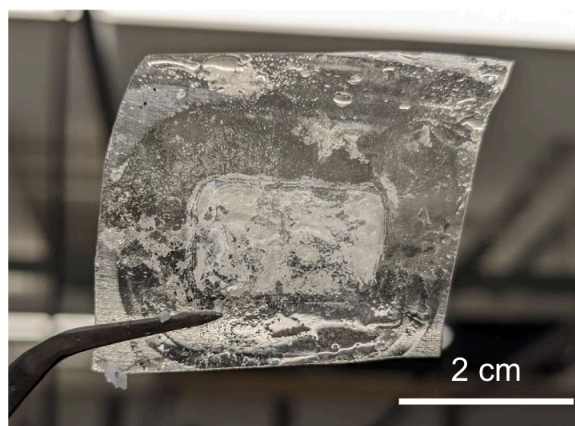


Figure S4. Optical photo of a Nafion™ 117 membrane after electrolysis. Noticeable $\text{Ca}(\text{OH})_2$ precipitate was found on its surface.

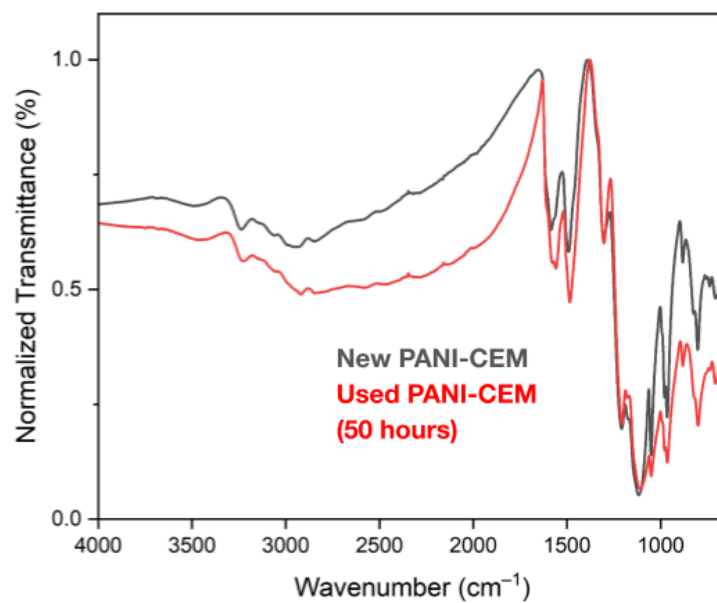


Figure S5. FTIR spectra of a PANI-coated Nafion™ 117 CEM that was new (grey) and after 50 hours of electrolysis (red).

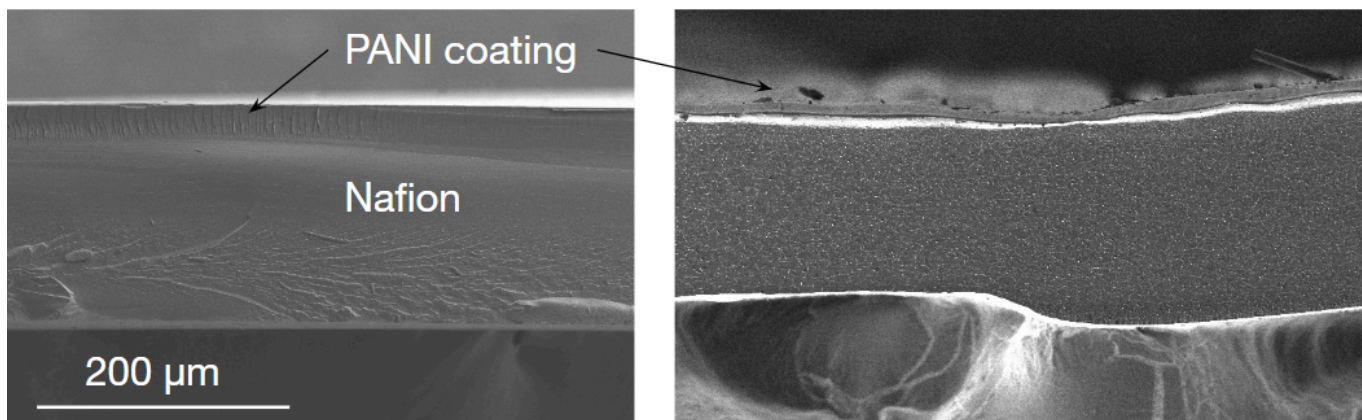


Figure S6. SEM cross-sections of the PANI-coated NafionTM 117 CEMs before (left) and after 50 hours of electrolysis (right).

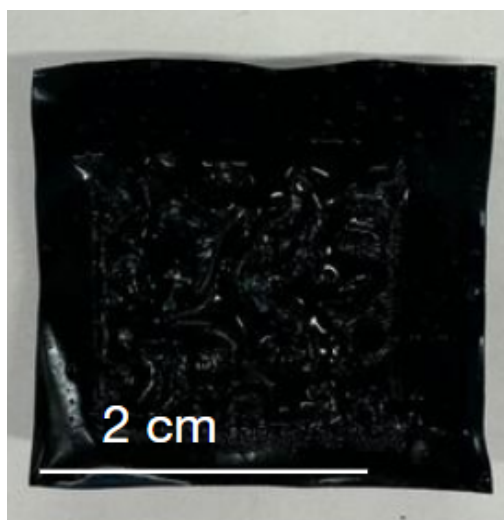


Figure S7. Digital photo of the PANI/CEM after a 50-hour electrolysis experiment.

(a)



(b)

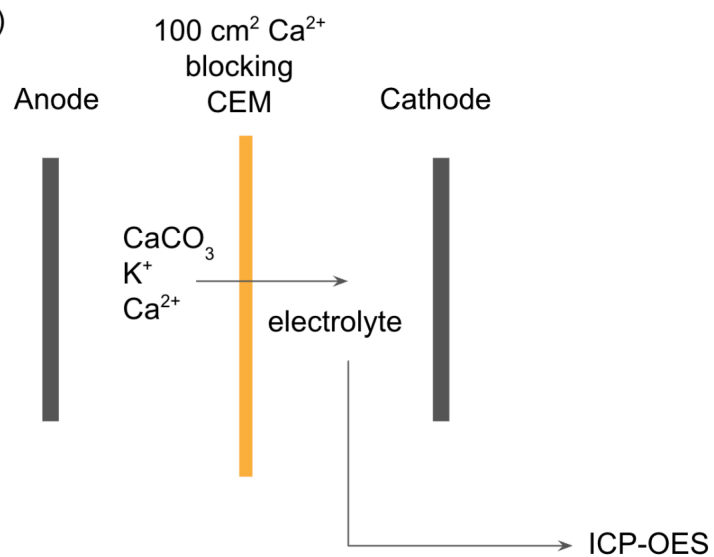


Figure S8. Optical photo of a $10 \times 10 \text{ cm}^2$ (active area) electrolyser. For the Ca^{2+} blocking selectivity test, 0.05 M CaCl_2 in 1 M KCl solution with excess CaCO_3 was fed into the anode, and the catholyte was collected every 30 minutes for ICP-OES test to determine the $[\text{Ca}^{2+}]$ for two hours of continuous electrolysis.

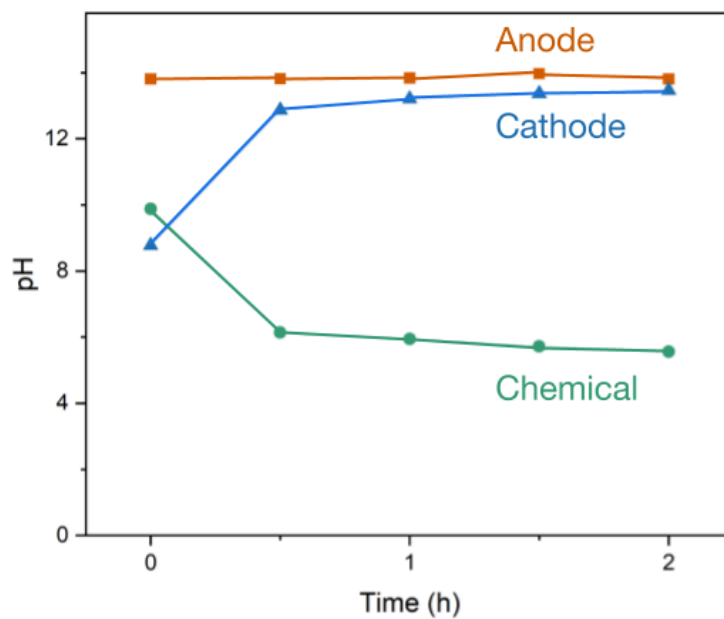


Figure S9. pH in the anode, cathode, and chemical compartments during a two-hour electrolysis experiment was measured using a pH probe. The anode and chemical compartments were separated by a Fumasep FBM bipolar membrane oriented in reverse bias, and the chemical and cathode compartments were separated by a NafionTM 117 cation exchange membrane with a polyaniline coating.

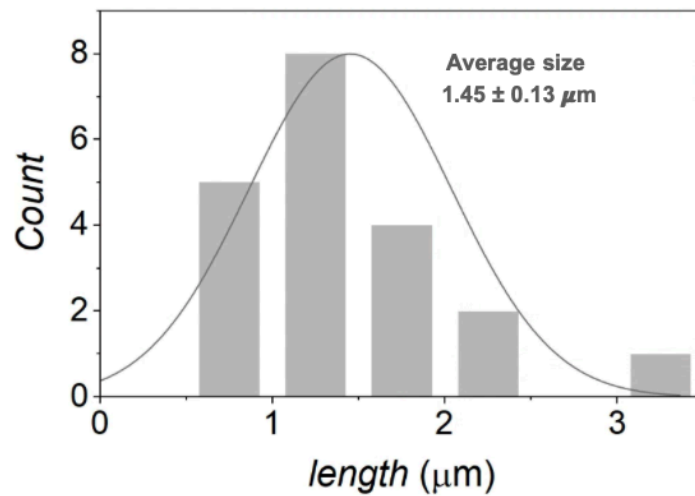
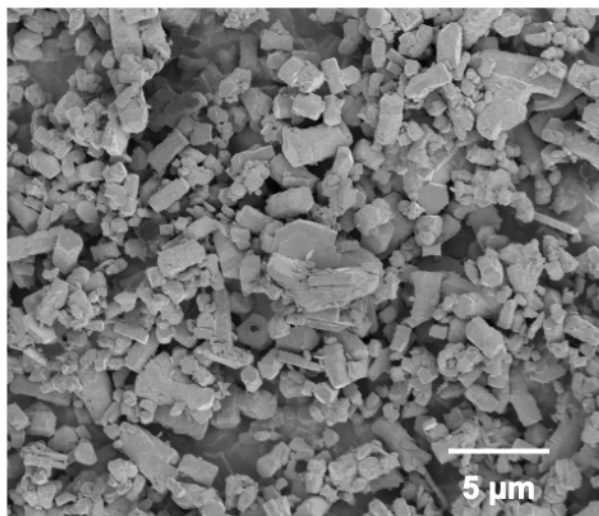


Figure S10. SEM (left) and size distribution (right) of the Ca(OH)₂ precipitates.

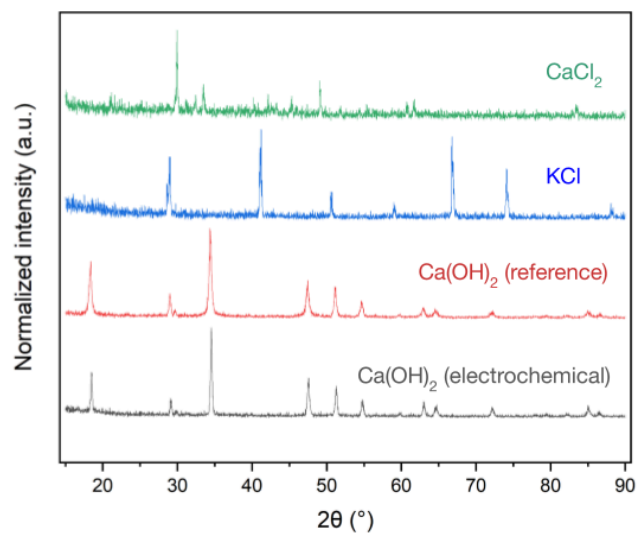


Figure S11. pXRD diffractograms of electrochemical Ca(OH)₂ product (grey), Ca(OH)₂ reference (red), KCl reference (blue), and CaCl₂ reference (green).

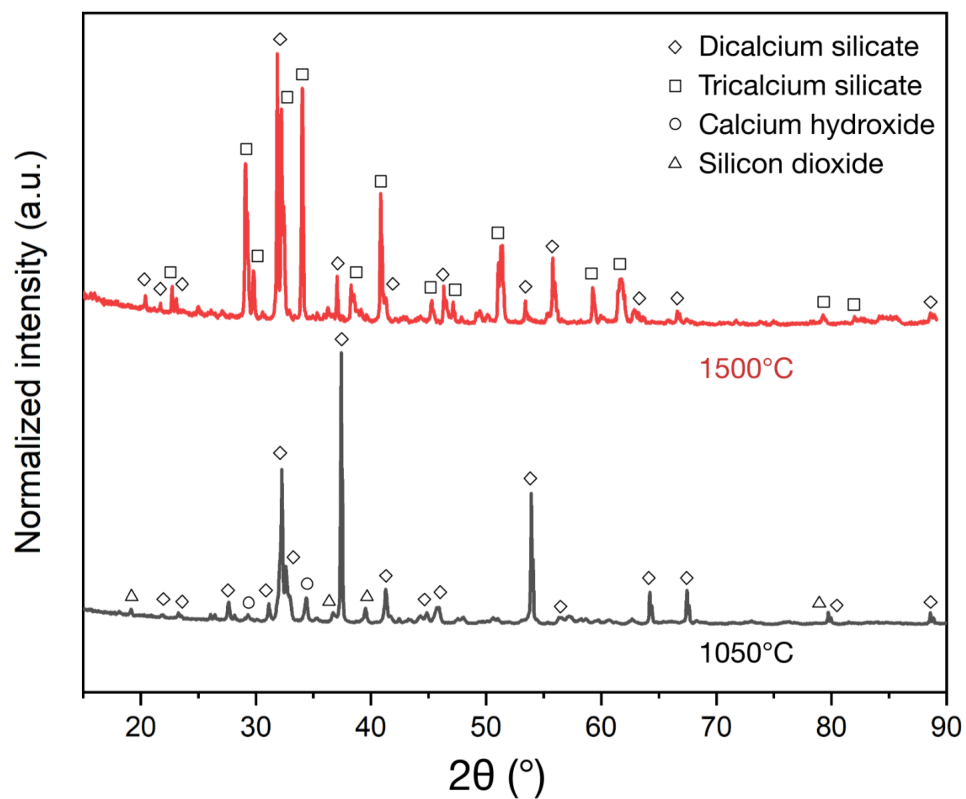


Figure S12. pXRD diffractograms of electrochemical $\text{Ca}(\text{OH})_2$ heated with SiO_2 to 1,050 °C (grey, bottom), and 1,500 °C (red, top). The heating and cooling rates were both 5 °C min^{-1} , and the kiln was held at the maximum temperature for 2 hours. Significant peaks are assigned as either dicalcium silicate ($2\text{CaO}\cdot\text{SiO}_2$),⁴ tricalcium silicate ($3\text{CaO}\cdot\text{SiO}_2$),⁵ calcium hydroxide ($\text{Ca}(\text{OH})_2$), depicted in Figure S10), and silicon dioxide (silica powder, SiO_2).⁶



Figure S13. The optical photo of the *operando* imaging system. The imaging system consisted of a modified two-compartment electrolyser with an open cathode compartment so we could image the CEM through the transparent catholyte with a high-resolution single-lens reflex (SLR) camera fixed above the electrolyser.

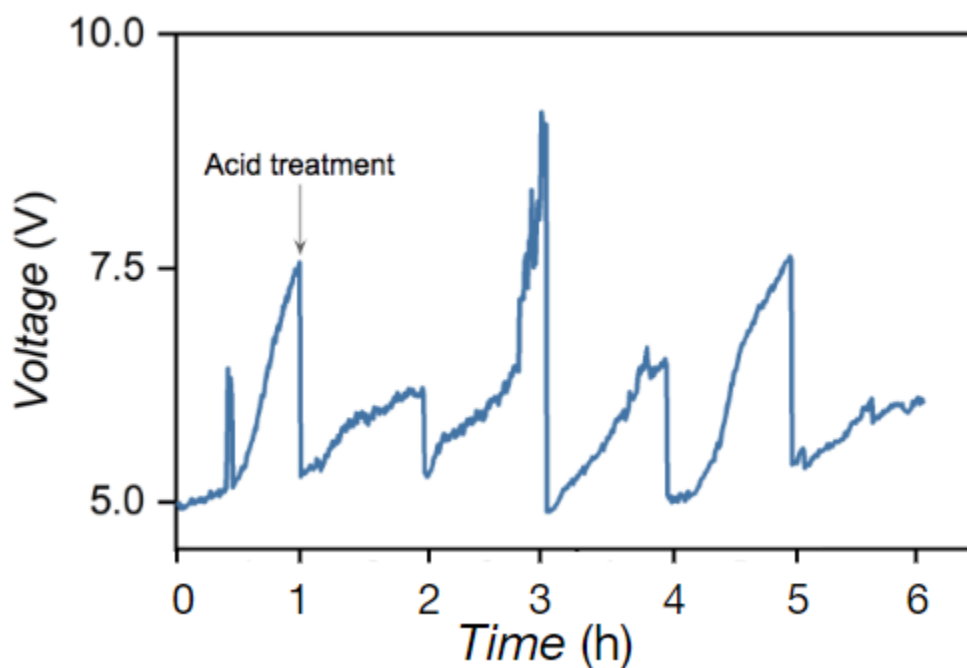


Figure S14. V_{cell} changes before and after acid treatment for the deposit removal. We performed cement electrolysis with a pristine NafionTM 117 CEM, and we recorded V_{cell} over time. The electrolyser was stopped, and the electrolyte at the cathode compartment was drained every hour after a significant increase in V_{cell} . Then 1 M HCl was circulated to the cathode compartment to remove the $\text{Ca}(\text{OH})_2$ on the NafionTM (facing cathode). This acid treatment can bring V_{cell} to the original voltage for multiple cycles. This result proved the deposit effect is reversible.

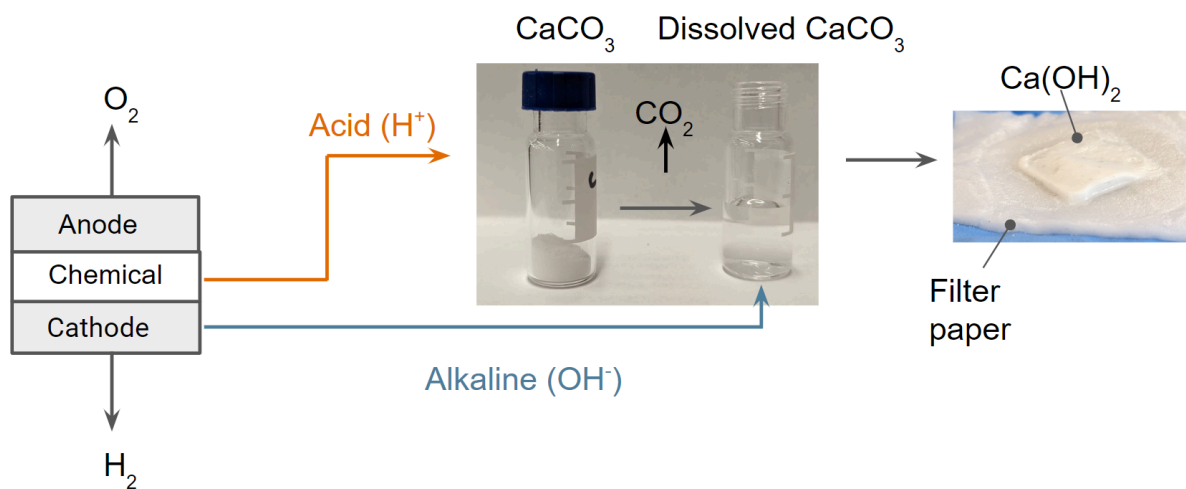


Figure S15. Electrochemical cement production using acid and base generated by an electrolyser. In this scenario, $CaCO_3$ is not directly fed into the electrolyser but reacts with the acid and base in sequence in a separated reactor — $CaCO_3$ decomposes when reacting with acids and releases Ca^{2+} , and it can be subsequently converted into $Ca(OH)_2$ with additional bases.

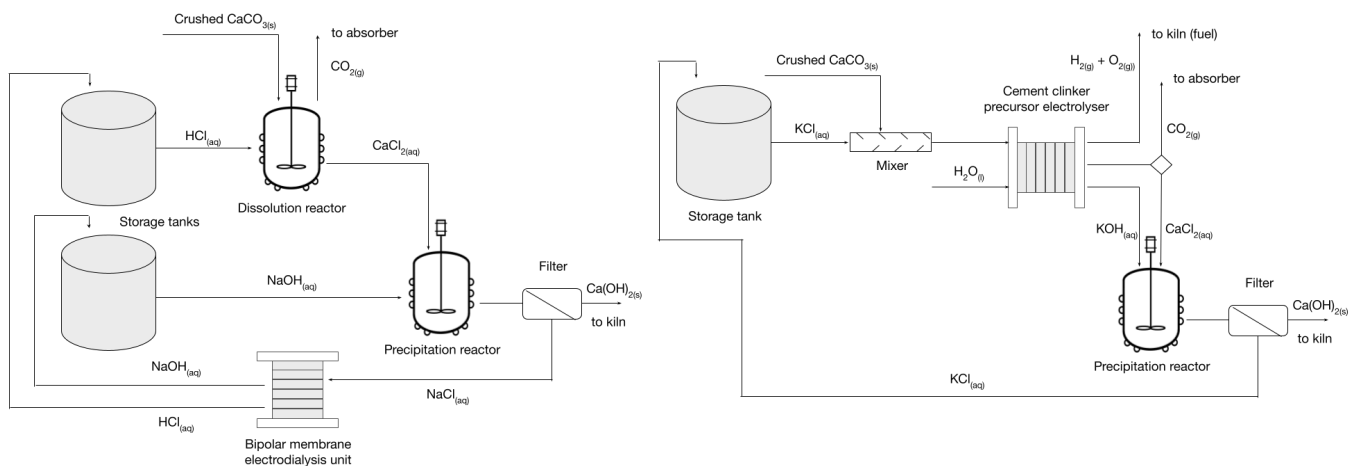


Figure S16. Comparison of two processes where CaCO₃ is dissolved in acid and precipitated with base. In the three-pot system (left), HCl and NaOH are added sequentially to the crushed CaCO₃, generating Ca(OH)₂, which is filtered out of the NaCl solution. This saltwater solution is passed through a bipolar membrane electrodiagnosis unit to regenerate the HCl and NaOH. In our two-pot system (right), supporting KCl electrolyte is mixed with crushed CaCO₃ to make a slurry, which is then fed into the electrolyser. The CaCO₃ dissolves in the chemical compartment of the electrolyser, releasing CO₂ and generating a CaCl₂ solution. The electrolyser also produces a stream of KOH from the hydrogen evolution reaction occurring at the cathode. This KOH stream is mixed with the CaCl₂ solution in a precipitation reactor to form Ca(OH)₂, which is filtered out of the KCl stream and sent to a kiln for conversion into CaO. The KCl can be reused as a supporting electrolyte without further treatment.

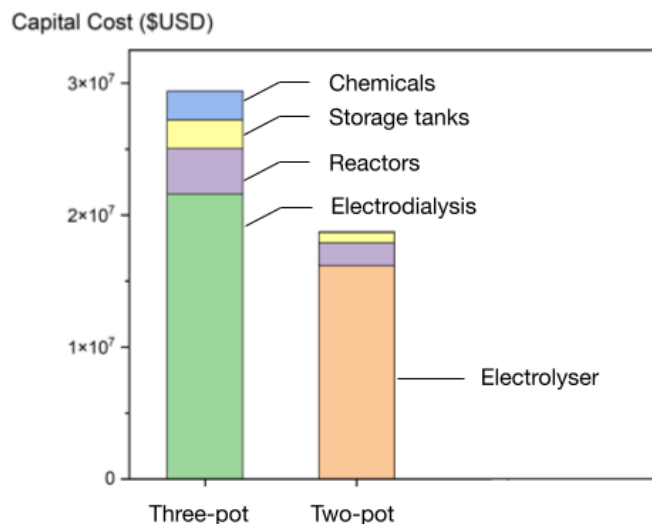


Figure S17. Techno-economic comparison of the capital costs of the two processes that dissolve CaCO_3 and precipitate Ca(OH)_2 is shown in Figure S16. Both processes are sized for a production capacity of 3,000 tons of cement per day. Only major process units and initial costs of chemicals are considered in this estimate.

The largest capital expense for the three-pot system (left) is an electro dialysis process to recover NaOH and HCl from the precipitation reactor. The cost is estimated based on a bipolar membrane electro dialysis unit that was modeled for the recycling of acid and base from the waste stream of a metallurgical process operating at the same scale as the hypothetical plant.⁷ It is necessary that the three-pot process recycles the acid and base from its waste NaCl stream. Without recycling, the process would require inputs of 2,409 and 2,642 tons per day of HCl and NaOH. This would have a daily cost of \$1.1 M USD.^{8,9} There would also be an enormous amount of salty wastewater being generated that would need disposal, incurring additional costs. The three-pot process also requires two large storage tanks (floating roof design, carbon steel construction) and two CSTR reactors (vertical orientation, stainless steel construction) with an estimated direct field cost of \$5.5 M USD.¹⁰ The total CAPEX for the three-pot process is then estimated to be \$29.4 M USD.

The integrated two-pot system (right) eliminates one storage tank and one reactor, which reduces the direct field cost to approximately \$2.5 M USD.^{10,11} The two-pot system also uses $\text{KCl}_{(aq)}$ as a supporting electrolyte, which is regenerated in the precipitation reactor and can be reused without further treatment, and is used at a much smaller scale than the HCl and NaOH required in the three-pot process. The largest capital expense of the two-pot system is the electrolyser, for which the cost was estimated based on a predicted future price of \$88 USD/kW for a PEM electrolyser,¹² and a power demand of 184.4 MW, consistent with the optimistic case where cell voltage is 2.5 V.¹³ This leads to an electrolyser capital cost of \$16.2 M USD. We use predicted future costs in this analysis because a cement plant incorporating our technology will not feasibly be constructed until the end of the decade at the earliest, while electro dialysis is a mature and well-studied technology.¹⁴

Table S1. Theoretical and measured $[\text{Ca}^{2+}]$ in the catholyte after one hour of electrolysis compared to $[\text{Ca}^{2+}]$ in the chemical compartment (Fig. 3). $[\text{Ca}^{2+}]_{\text{theoretical value}}$ was calculated using eqn (S2) and $[\text{Ca}^{2+}]_{\text{catholyte}}$ was measured via ICP-OES. The charge carried by K^+ was calculated using eqn (S1).

$[\text{Ca}^{2+}]_{\text{chemical}}$ (M)	$[\text{Ca}^{2+}]_{\text{theoretical value}}$ (mM)	$[\text{Ca}^{2+}]_{\text{catholyte}}$ (mM)	Charge carried by K^+ (%)
0.05	7.46	0.025 ± 0.002	99.7 ± 6.2
0.50	7.46	0.070 ± 0.002	99.1 ± 2.9
1.00	7.46	0.099 ± 0.003	98.7 ± 3.0

Table S2. Theoretical and measured $[\text{Ca}^{2+}]$ in the catholyte over 50 hours of electrolysis (Fig. 3). $[\text{Ca}^{2+}]_{\text{theoretical value}}$ was calculated using eqn (S2), and $[\text{Ca}^{2+}]_{\text{catholyte}}$ was measured via ICP-OES. The charge carried by K^+ was calculated using eqn (S1). The catholyte was refreshed after the 24 h aliquot was collected.

Time (h)	$[\text{Ca}^{2+}]_{\text{theoretical value}}$ (mM)	$[\text{Ca}^{2+}]_{\text{catholyte}}$ (mM)	Charge carried by K^+ (%)
1	7.46	0.093 ± 0.005	98.8 ± 5.4
5	37.3	0.131 ± 0.002	99.6 ± 1.5
24*	179	3.42 ± 0.01	98.1 ± 0.3
32	59.7	1.84 ± 0.11	96.9 ± 6.0
50	194	2.61 ± 0.06	98.7 ± 2.3

* Catholyte was refreshed after this measurement

References

- 1 H. Farrokhzad, M. R. Moghbeli, T. Van Gerven and B. Van der Bruggen, *React. Funct. Polym.*, 2015, **86**, 161–167.
- 2 A. L. Smith and S. E. Stein, in *NIST Chemistry WebBook, NIST Standard Reference Database Number 69*, ed. P.J. Linstrom and W.G. Mallard, National Institute of Standards and Technology, Gaithersburg MD, 1982, 1–24.
- 3 Timothy J. Johnson, Tanya L. Myers, Yin-Fong Su, Russell G. Tonkyn, Molly Rose K. Kelly-Gorham, and Tyler O. Danby, in *NIST Chemistry WebBook, NIST Standard Reference Database Number 69*, ed. P.J. Linstrom and W.G. Mallard, National Institute of Standards and Technology, Gaithersburg, MD, 2023.
- 4 S. Udagawa, K. Urabe, M. Natsume and T. Yano, *Cem. Concr. Res.*, 1980, **10**, 139–144.
- 5 F. Nishi, Y. Takeuchi and I. Maki, *Z. Kristallogr. Cryst. Mater.*, 1985, **172**, 297–314.
- 6 Z. An, H. Wang, C. Zhu, H. Cao and J. Xue, *J. Mater. Sci.*, 2019, **54**, 2787–2795.
- 7 Kuldeep, W. D. Badenhorst, P. Kauranen, H. Pajari, R. Ruismäki, P. Mannela and L. Murtomäki, *Membranes*, 2021, **11**, 718–731.
- 8 BusinessAnalytiq, Hydrochloric acid price index, <https://businessanalytiq.com/procurementanalytics/index/hydrochloric-acid-price-index/>, (accessed 1 February 2024).
- 9 BusinessAnalytiq, Sodium hydroxide price index, <https://businessanalytiq.com/procurementanalytics/index/sodium-hydroxide-price-index/>, (accessed 1 February 2024).
- 10 R. H. Perry, D. W. Green and J. O. Maloney, Eds., *Perry's Chemical Engineers' Handbook*, McGraw-Hill, Seventh Edition., 1997.
- 11 D. Mody, *ChemEcon: Chemical Plant Costing & Economic Analysis*, Queen's University, 2017.
- 12 S. Krishnan, V. Koning, M. Theodorus de Groot, A. de Groot, P. G. Mendoza, M. Junginger and G. J. Kramer, *Int. J. Hydrogen Energy*, 2023, **48**, 32313–32330.
- 13 B. A. W. Mowbray, Z. B. Zhang, C. T. E. Parkyn and C. P. Berlinguette, *ACS Energy Lett.*, 2023, **8**, 1772–1778.
- 14 R. Pärnamäe, S. Mareev, V. Nikonenko, S. Melnikov, N. Sheldeshov, V. Zabolotskii, H. V. M. Hamelers and M. Tedesco, *J. Memb. Sci.*, 2021, **617**, 118538.